

Analysis of low latitude Noctilucent Cloud occurrences using satellite data and modeling

James M. Russell III, P. P. Rong, M.E. Hervig, S.M. Bailey, J. Gumbel, A. Lambert

Abstract

Numerous NLC sightings have occurred in recent years at latitudes as low as $\sim 40^{\circ}\text{N}$ in the skies over Chicago, Illinois, Boulder, Colorado, Omaha, Nebraska, Logan, Utah, Seattle, Washington, Calar Alto, Spain and Paris, France. While no confirming evidence has come forth thus far, such sightings raise the natural question about whether there are systematic NLC increases occurring at these low latitudes. This question is investigated using observations of temperature made by the SABER instrument on the TIMED satellite over the 2002 to 2011 time period, a 7-year water vapor climatology developed from data collected by the MLS instrument on the Aura satellite for 2005 to 2011, and Polar Mesospheric Cloud (PMC) measurements made by the OSIRIS instrument on the Odin satellite for the 2002 to 2011 period. These data are used in conjunction with a 0-D thermodynamic equilibrium model [Hervig et al., 2009] that assumes mesospheric ice is in equilibrium with available water vapor. All analyses were performed on the 0.00464 hPa surface or ~ 84 km, which is the northern hemisphere mean cloud height. Both MLS 0-D and OSIRIS measured PMCs agree well with the SABER 0-D results for 2005 to 2011. Results show a statistically significant upward trend in the number of 0-D derived PMCs per season in the latitude range 40° - 55°N for 2002 – 2011. The long-term increases in cloud number are considered being driven by the corresponding temperature decreases over the same time period. Solar cycle effects have not yet been removed in this analysis.

1. Introduction

In recent years mesospheric clouds (PMCs), or noctilucent clouds (NLCs), have been more frequently observed in latitudes lower than 50°N . For example, the space-weather archived NLC gallery shows that during June and July of 2003, 2007, 2008, and 2009 there were a number of cloud sightings photographed in the US towns in Washington State ($47.2\text{-}48.5^{\circ}\text{N}$), Minnesota (46.8°N), Montana (45.2°N), Oregon ($44\text{-}46.2^{\circ}\text{N}$), South Dakota (44.5°N), Wyoming ($42.9\text{-}43.5^{\circ}\text{N}$), Nebraska (41.5°N), and Colorado (40°N). These latitudes are outside the zonal circle that separates the regular PMC region and the mid-latitude region (Figure 1), and the records are very rare prior to 2007. The number of occurrences in 2009 is significantly larger than in the previous years and furthermore 2009 is the only year among four in which there was a sighting in Colorado on latitude 40°N . More drastically, in mid-June 2012 NLCs were observed at Carla Alto Observatory at 37.2°N . However, we should note that most of the NLC sightings were reported by individual observers and the data were not collected on a regular basis for any given site. This leaves room for uncertainties, for example, prior to 2007 the NLC occurrences may have been more often but were less reported. Wickwar et al. [2002] reported a NLC display in June 1999 in Logan, Utah (41.7°N). At the same night NLCs were also reported at Golden, Colorado (39.8°N). Early records about the low-latitude NLCs can be traced back to June 1963 when Meinel et al [1963] photographed some bright noctilucent clouds north-west of Tucson (32°N). However, these clouds were thought to be caused by a rocket vehicle launch, and therefore most probably is a result of an in-situ water vapor (H_2O) enhancement.

It is highly probable that these individual observations do indicate that low-latitude mesospheric clouds are increasing, and this may further imply that mesospheric temperature and H_2O are changing over the last decade or so. The mechanism of the 2009 low latitude cloud

outbreak was however interpreted as being caused by the anomalous dynamical conditions; Neilsen et al. [2011] argued that such an outbreak is a result of the 5-day planetary wave anomaly, combined with a wind advection that transports the clouds southward. Nevertheless, the fact that these sightings also occurred in 2003, 2007, 2008, and 2012 on increasingly lower latitudes indicates that these NLC sightings might suggest more fundamental change of the mesosphere rather than just a series of anomalous events. In this study we used both model simulations and data analysis to make attempt to answer several important questions, such as, whether mesospheric T or H₂O was changing over the last decade? If such a change did occur, does it extend over the entire polar region? What controls the frequency change of the low-latitude mesospheric clouds? Is the PMC frequency changing north of 50°N? Is the conclusion going to change when dimmer or brighter clouds are analyzed exclusively?

The mesospheric cloud frequency trends were studied previously but the conclusions are not consistent. For example, using UK and Denmark records during 1965-2005, Kirkwood et al. [2008] found no significant trend in the overall cloud frequency, but a significant upward trend was reported for the brighter clouds. Gadsden [1998] used 40 years (1958-1998) records of North-West Europe (50°-58°N, mainland Scotland and Denmark) and found significant upward trend. In Gadsden [1998] “North-West” Europe refers to the longitude range of 11°W-20°E, which should include UK as well, but their conclusions do not agree. This suggests that slightly different locations or any inconsistencies in the data collection or data analyzing approach could affect the calculated trend. In this study we will use modeled mesospheric clouds to calculate the cloud number decadal trend, and to examine the relationship between the cloud number and T or H₂O. Relative to using only the PMC data, a model study will provide firmer theoretical standpoint which may assist resolving the inconsistencies between different cloud datasets. In

addition, the gridded data points in the model simulations will eliminate the disadvantages of individual observing sites because the entire PMC region is evenly covered.

The PMC trend is expected to be associated with the corresponding temperature or H₂O trend since the latter two are the most important factors that determine the cloud frequency and mass density variations. Obtaining the long term trend of T and H₂O in the mesosphere is extremely challenging because it requires multi-decadal datasets that extend into the upper atmosphere, and so far only a few datasets meet such standards. Furthermore, the temperature and H₂O trend may vary with season, latitude, and altitude. In addition, the length of the time series is also important because the trend varies as the time window shifts forward or backward. A summary on some of the previous trend studies were given by Beig et al. [2003]. Despite the significant discrepancies in the magnitude of the trend most of these studies point to an overall cooling mesosphere although various time periods and latitude ranges were used in different studies. For example, using the falling sphere and rocket grenade dataset, Lübken et al. [2000] found an extremely weak cooling trend, i.e., -0.24 ± 0.14 K/decade, at Alomar (69°N, 10°E), over the time period 1987-2000 in altitude range 50-85 km. The authors also claim that there is no clear solar cycle effect being noted or removed. Remsberg [2009] used HALOE data (1991-2005) [Russell et al., 1993] to extract a global-wise cooling trend, i.e., $\sim 1-3$ K/decade in latitude range 40°S-40°N, in the upper stratosphere to mesosphere up to 80 km altitude. The solar cycle effect was clearly noted and separated before the linear trend is calculated. It was found in this study that the solar effect is in a similar magnitude to the linear trend, in which case we should always be cautioned about what trend is under discussion, before or after the solar cycle removal. Whole Atmosphere Community Climate Model (WACCM) temperature trend for years 1950-2003 also indicates a systematic cooling of 0.5-1.0 K/decade in altitude range 20-100 km altitude

[Garcia et al., 2007]. However, using Leibniz-Institute Middle Atmosphere Model (LIMA) model results, Berger and Lübken [2011] drew a slightly different conclusion. They calculated the summer mesospheric trend for the last 5 decades (1961–2009), and found that during 1979-1997 there is a cooling trend of 3-5 K/decade at all latitudes, but during 1997-2009 it is a 1-2 K/decade warming trend especially for the northern hemisphere mid-high latitude region. Such a result would contradict a low latitude cloud number increase in the recent decade but we should note that these trend values are obtained after the solar cycle effect has been removed. If what they found is correct then the cloud number increase in the recent decade is entirely caused by solar cycle. The mesospheric H₂O trend is even harder to obtain because very few datasets had H₂O product retrieved in the mesosphere. Remsberg [2010] showed that HALOE H₂O in the mesosphere has a consistent upward trend in latitude range 40°S-40°N, and the trend increases as latitude increases, with a maximum of ~15%. In the same paper it also showed that the magnitude of the solar cycle effect reaches ~20-30%, far exceeding the long term trend. The percentage of the solar cycle effect roughly agrees with what Hervig and Siskind [2006] have found at 80 km altitude from HALOE data analysis although the latter analysis was performed in latitude range 65°-70°N. This again indicates that incomplete solar cycle removal can significantly affect the magnitude of linear trend. WACCM modeled multi-decadal H₂O trend in the mesosphere is consistently positive but the magnitude remains at ~3-4% on all latitudes including the polar region. One interpretation to the much larger trend in HALOE dataset may be the fact that HALOE H₂O has fairly poor precision in the upper mesosphere, which will lead to poor significance level of the trend.

Given the generally supported cooling and wetting trend in the mesosphere, in this study we will use SABER temperature and MLS temperature and H₂O to conduct the trend analysis on

the middle to high latitudes in northern summers, and to investigate whether these trends support the middle latitude cloud number increase over the last decade. We should point out that obtaining a long term linear trend is not the focus of this study, instead, we are mainly interested in finding a connection between the temperature or H₂O secular trend and the cloud number increase, and the trend should include both the long term and solar cycle components. This study differs from the previous trend studies in the sense that we used a cross-validation between clouds and the environmental variables through physical relations so that the result will be more reliable than using either set alone. It is also important to find out whether solar cycle signals are detectable on all latitudes, if not, how much the signal varies as the latitude increases.

2. Data sets used and the analysis approach

Sounding of the Atmosphere using Broadband Emission Radiometry (SABER/TIMED) v1.07 temperature [Remsberg et al., 2008], and MLS/Aura temperature [Schwartz et al., 2008] and H₂O [Lambert et al., 2007] are used to perform the 0-D simulations. All data events north of 40°N are included. For each event the pressure level 0.00464 hPa is chosen, which is approximately at 84 km and is roughly the centroid height of the PMCs. We chose the vertical level based on the MLS data registration because the vertical resolution of MLS data is many times poorer than that of SABER, which is about 15km vs. 2 km.

Optical Spectrograph and InfraRed Imager System (OSIRIS/Odin) PMC data [e.g., Petelina et al., 2006] is used to provide the observational support to the 0-D modeled cloud number inter-annual variability. OSIRIS PMC data is available from 2002 to the current time and is the only satellite dataset to date that has retrieved mesospheric clouds on latitudes lower than 50°N/S. Owing to its limb viewing geometry OSIRIS is more sensitive than a nadir instrument

such as Solar Backscattering Ultra Violet instrument series (SBUV) or Cloud Imager and Particle Size experiment (CIPS/AIM) [Benze et al., 2009], but only 20% of its measuring time is dedicated to the mesospheric mode and furthermore the number of events varies significantly with the year. Especially in years 2002-2004 the measurements are far too few to form any reasonable intra-seasonal variation. As a result, we are only able to use the data after year 2004.

The Spatial Heterodyne Imager for Mesospheric Radicals (SHIMMER/STPSat-1) PMC data [Stevens et al., 2009; Siskind et al., 2011] and The Advanced Level Physics High-Altitude (ALPHA) prototype of the Navy Operational Global Atmospheric Prediction System (NOGAPS) assimilated data, or NOGAPS-ALPHA data [Eckermann et al., 2009], are used to verify the local time dependence of PMCs and to validate the 0-D model. SHIMMER is a limb-viewing ultraviolet spectrometer that was launched in 2007 and ended its mission in 2009. Owing to its low-orbital inclination angle (35.4°) SHIMMER can take PMC measurements in fairly low polar latitudes such as 50° - 58° N/S. The Rayleigh scatter threshold chosen for PMC detection is about 100KNR/nm. The valid data points of PMCs cover about 5-7 hours of local time per day and the time window shifts as season progresses. In NOGAPS-ALPHA SABER v1.07 and MLS v2.2 temperatures up to 0.002 hPa are assimilated. NOGAPS-ALPHA provides regularly gridded (1° lon \times 1° lat) global analysis fields of geopotential heights, temperatures, H₂O and O₃ mixing ratios, horizontal winds, and other quantities every 6h at 60 reference pressure levels distributed roughly evenly in pressure height over the range 1000-0.0005hPa, and on four UT times per day. In this study the pressure level 0.0036 hPa is chosen as an approximate PMC height to perform the 0-D simulations. The fact that the NOGAPS-ALPHA data are given on the regular 3-dimensional grids enabled us to only simulate the 0-D clouds on the SHIMMER orbital tracks so that the total event number and the local times are matched. To make the local times match more

closely, the NOGAPS-ALPHA temperature and H₂O fields are linearly interpolated onto 23 UT hours prior to the 0-D simulations.

3. 0-D model

0-D model was first proposed by Hervig et al. [2009] and proves to be highly effective in reproducing the intra-seasonal variation of the cloud frequency and ice mass density [also see Rong et al., 2012]. In 0-D model it was hypothesized that a 100% H₂O that is in excess of the saturation vapor pressure (P_{SAT}) is turned into ice, and a simple thermal equilibrium exists between the vapor and ice phases. It highlights the macro-physical relationship between the bulk ice and the environmental temperature and H₂O, and ignores the detailed micro-physics such as the nucleation process and the dynamical processes such as upwelling and advection transport of H₂O. 0-D model works well because the microphysical responding time of cloud genesis to the prevailing temperature and H₂O is as short as a few hours, and therefore longer time scale processes such as upwelling or planetary waves will change temperature, H₂O, and the bulk ice approximately the same time and not much time lags are expected. However, an in-situ fast advection (~30m/s) can blow the clouds several hundred kilometers downstream without having to change temperature or H₂O condition [Baumgarten et al., 2012]. In addition, when temperature is closer to the frost point the nucleation barrier is stronger and the misrepresentation of the ice mass may be more severe than under the strongly saturated condition.

In this study 0-D model will be used as a primary tool to diagnose the mesospheric cloud number variation in all latitude ranges throughout the last decade, and therefore how well it reproduces the cloud number variation is critically important, for example, on the intra-seasonal and inter-annual scales. We should point out here that cloud number and cloud frequency are

virtually the same problem in the PMC study because the daily total event number varies only slightly in datasets such as SABER, MLS, and NOGAPS-ALPHA. The reason we prefer to adopt cloud number rather than cloud frequency is because in latitude range 40° - 60° N the cloud number is very low in relative to the total event number so that the frequency becomes an inconveniently small number.

Figure 2 shows the intra-seasonal variation of the cloud daily frequency in latitude range 40° - 85° N for each year from 2005 to 2011 for OSIRIS PMC data and 0-D clouds, respectively. The 0-D clouds are calculated using MLS temperature and H_2O . We note strong agreement between the model and observation, on both the variation rhythm and the magnitude. However, the OSIRIS time series shows occasional spikes in 2007 and also there are some missing days in 2005 and 2006. Given the global coverage and the relatively high sensitivity to weak PMCs, OSIRIS should be an ideal dataset to study many aspects of the PMCs, but its highly fluctuating event number from year to year hinders its potential usage, especially during the first few years after its launch.

Comparing the 0-D results with SHIMMER PMCs tests the model ability to simulate the local time dependence and inter-annual variability. SHIMMER stands out from other satellite instruments because it is not on a sun-synchronous orbit and therefore the local time dependence of PMCs can be studied. In addition, the PMC measurements in SHIMMER, which is about ~ 300 events per season, are exclusively taken in the lower polar latitude range (50° - 58° N) and therefore more reliable statistics can be obtained. In comparison, OSIRIS detects about ~ 20 cloud events per season in the same latitude range. NOGAPS-ALPHA T and H_2O are used in the 0-D simulations, and are interpolated onto 23 hours with 1-hour increment as mentioned above. Figure 3 shows the comparison between the 0-D (left) and SHIMMER (right) daily cloud

number for years 2007-2009 respectively. Three threshold values for m_{ice} is used, i.e., 0.0, 25, 40 ng/m^3 , are used, and apparently as the threshold increases the cloud number reduces, but the intra-seasonal variation shows strong qualitative agreement with the SHIMMER cloud number in all three years. The strong agreement suggests that local time variation in NOGAPS-ALPHA and SHIMMER show consistency via model cloud physics. However, it is noted that the cloud number in 0-D is generally larger than in SHIMMER, and the threshold 40 ng/m^3 drew the two results closer. This does not necessarily mean that SHIMMER is not sensitive enough. Rather, the extended coldness shown in the NOGAPS-ALPHA temperature from polar to the mid-latitude region might be the problem. This is most likely caused by the involvement of MLS temperature in the NOGAPS-ALPHA assimilation scheme. For example, Rong et al. [2012] has shown that the mean MLS temperature in the polar mesospheric region has a ~ 10 K cold bias with respect to the SOFIE counterpart. Another point worth noting is that it is hard to pick one appropriate threshold under which the 0-D modeled and SHIMMER observed cloud numbers agree well in all aspects. For example, in 2009 when 40 ng/m^3 is taken as the threshold the cloud number magnitudes are closer, but the 0-D result exhibits too drastic of a difference between the first and second halves of the season. In comparison, the result with a zero threshold is more reasonable in this regard although their overall cloud numbers are six times apart. This suggests that it requires more advanced understanding of the cloud physics and dynamics to further improve the modeling capability.

4. Decadal trend of cloud number and temperature

We next examine the decadal trend of the 0-D mesospheric cloud number in different latitude ranges, with the lower-latitude range (40° - 50°N) being the focus of the discussion. For each season the total number of 0-D clouds (N) is obtained, and then it is normalized by its 10-

year average. The normalized cloud number, denoted by N_{norm} , is the primary variable used in this study.

Prior to describing the model results, the H₂O climatology used in the model simulations is discussed. In each 2°lat bin and for each given day, the zonal maximum (Figure 4upper-left) and mean value (Figure 4upper-right) of MLS H₂O are calculated over its 7-year mission period, respectively. The horizontal axis is days from summer solstice (DFS), and the climatology is calculated for the individual DFS. In the 0-D simulations the zonal maximum climatology is used because the ideal H₂O input for the 0-D model should be the one with the least depletion feature. Note that the majority of the retrieved polar H₂O profiles at the PMC height will exhibit depletion feature owing to PMC production, as is clearly seen in Figure 2upper-right. However, we should point out that if both weak and strong clouds are accounted for, the cloud number or appearance frequency is not sensitive to the H₂O variation [Rong et al., 2012]. But the conclusion will change if bright clouds are counted exclusively. The yearly H₂O variations and secular trends in different latitude bands from 40°N to 85°N, with a 5-degree increment, are shown in the lower two panels of Figure 4. The lower-left panel is for time period 1st May - 31 August, and the lower-right panel is for the core of summer that extends from the solstice to about 25 days after solstice. Both cases show consistent results, indicating a strong inter-annual variability and an upward trend that becomes more significant as the latitude increases. Although the confidence levels of these trends are generally poor, they support an increased number of high latitude bright clouds over the years, which will be discussed in section 7.

The time series of N_{norm} , shown in Figure 5, indicate an upward trend with high confidence levels in the SABER analysis in latitude range 40°-55°N, while in higher latitudes the upward trend reduces and especially in latitudes north of 70°N the number of clouds shows

negligible changes over the years. The zero-trend in the high polar latitudes is expected because the cloud frequency is nearly 100% and the total event number per year is almost unchanged. The MLS results show strong agreement with SABER in years 2005-2011 although different H₂O conditions are used in the two analyses. This suggests that temperature is the main driver of the low-latitude cloud number change. In the latitudes north of 70°N, the trend in both analyses approaches zero but the shorter term variability is stronger in SABER. Figure 6 shows a similar set of time series except that N_{norm} is further adjusted by the ratio of the current year total event number and the multi-year averaged event number, denoted by N_{norm_adj} . The variable N_{norm_adj} is equivalent to yearly cloud frequency. Although the total event number per year varies only by a small fraction in both SABER and MLS datasets, they will have some minor effect on the results. The time series in Figure 6 show roughly the same features as in Figure 5, which verifies a previous argument that cloud number and frequency are virtually the same description of PMCs and the variations of both are controlled by the same physics. However, after adjustments are made the fluctuations in the SABER analysis are generally reduced; such a reduction is especially notable in the polar latitudes north of 70°N, leading to better agreement between the two analyses.

OSIRIS PMC data in 2005-2011 are used to validate the inter-annual variability of the 0-D cloud number in the low latitude ranges, shown in Figure 7 upper panels. Since OSIRIS cloud number is overall about 20 times fewer than the 0-D clouds the actual cloud numbers have to be normalized to do the comparisons; the cloud number is first subtracted by its multi-year mean and then divided by the standard deviation. Cloud numbers in higher latitudes are not compared because the cloud frequency is close to 100% and the fluctuations are random noises. Figure 7 upper panels show that OSIRIS and 0-D results agree well. In Figure 7 lower panels the inter-

annual variations of normalized cloud numbers are shown for both OSIRIS and the 0-D results; in particular, N_{norm_adj} is used in the OSIRIS analysis because we have known from above that OSIRIS event numbers are highly uneven for different years. For example, in 2005 and 2006 the event numbers are several times fewer than in the later years. Both OSIRIS and 0-D results indicate that as latitude increases the inter-annual variability is reduced and in polar latitudes they are simply “flat”. As discussed above, the “flat” curves in the polar latitudes are expected, but a slight “bending-up” feature is noted in the OSIRIS result, which is likely unrealistic and is the residual effect of the uneven yearly event numbers. Figure 7 indicates a good qualitative agreement between OSIRIS PMC data and the 0-D results, which lends support to the reliability of 0-D model on simulating longer time scale variabilities. Speaking of trend, although the OSIRIS time series has also shown a hint of upward trend in latitude range 45°-55°N, they are not statistically significant. Longer PMC records will assist to verify such a trend.

We argued above that temperature is the main driver of the low latitude cloud number increase, and some previous studies also supported this argument [e.g., Fiedler et al., 2011; Rong et al., 2012]. For example, Rong et al. [2012] suggested that when temperature is close to the frost point it fully controls the frequency variation, while when it is far below the frost point the frequency is close to 100% and is insensitive to any further temperature decrease.

Figure 8 shows the yearly time series of the temperature anomaly for SABER and MLS. The anomaly is obtained by subtracting the 10-year mean (7-year for MLS) from the yearly data. For any given year and latitude band (e.g., 40°-45°N), the yearly temperature is obtained through averaging all temperature values on the 0.00464 hPa surface throughout the period 1st May - 31 August. Although we realize that PMCs first appear around mid-May, 0-D clouds usually occur much earlier especially when using the MLS data to do the simulations. Figure 8 indicates a

significant cooling trend in latitude range 40° - 55° N, with a high confidence level of ~ 80 - 95% ; the strongest trend reaches -0.3 ± 0.16 K/yr and then reduces as the latitude increases. The inter-annual variability of temperature is roughly anti-correlated with the normalized cloud number variations shown in Figures 5 and 6, supporting the temperature control of the cloud number variation. Furthermore the agreement between SABER and MLS is excellent, although in latitudes north of 65° N SABER exhibits stronger inter-annual variability. Stronger fluctuations in SABER temperature is not surprising because SABER captures more small scale structures attributed to its fine vertical resolution. Solar cycle effect is another important varying mode to examine in these yearly time series. Although inter-annual variability is fairly strong in these analyses, it appears that on latitudes lower than 55° N the variation does somewhat follow the solar cycle, for example, 2009 is the solar minimum and meanwhile is the coldest year while after 2009 it started warming up. In the polar latitudes, on the other hand, barely any solar cycle signal is recognized. In fact, in the polar latitudes 2009 is the 2nd warmest year next to 2002. Such a discrepancy between polar and mid-latitudes can be a reflection of dynamics. For example, Neilsen et al. [2011] argued that 5-day planetary wave anomaly caused the outbreak of the cold temperature in Europe in 2009. In the real atmosphere it could be the combined effect of solar cycle and dynamics that led to the cold 2009 in the mid-latitude mesosphere. The solar cycle effect by itself is expected to be present ubiquitously, but the impact is likely decreased toward the polar latitudes. We are currently unable to provide any appropriate interpretation to such a latitudinal dependence of the solar cycle effect. In a previous study Hervig and Siskind [1996] used HALOE temperature to extract a clear solar cycle signal on latitude 67.5° N without much interference from the inter-annual variability. If compare the overlapped period from 2002

to 2005, we find that the results in Hervig and Siskind [2006] and the current study basically agree except that in the SABER analysis the cold anomaly in 2003 seems stronger than expected.

5. Yearly anomaly of temperature and cloud number within the season

After obtaining the yearly time series based on the whole-season average of temperature, we will next examine the same variability on the detailed stage-wise basis. The averages of temperature and cloud numbers are performed on the 8-day running windows, shown in Figure 9. The colored maps in Figure 9 are temperature anomalies only, and the fillings between the individual years are simply linear interpolations for better viewing effect. The histograms are temperature anomaly (rainbow) and the cloud number anomaly (pink) over-plotted. The cloud anomaly here refers to the anomaly of variable N_{norm} . When N_{norm} anomaly is positive, the cloud number is above the multi-year average level, and visa-versa. Three latitude bands, 40°-45°N, 65°-70°N, and 80°-85°N, are chosen to represent the middle to high latitude cases. The colored maps indicate that the magnitude of temperature anomaly is the strongest in the mid-latitude region, and then it weakens toward the polar region. Furthermore, if examining the high latitude band (80°-85°N) only, we find stronger anomalies at the start and end of the season. This suggests that warmer temperature, which is closer to the frost point, is more prone to variability and will further support the cloud number variability. We also note from these maps that the anomalous coldness in 2009 and the decadal cooling trend are primarily restricted to the time after the solstice, which corresponds to the mid-latitude mesospheric cloud outbursts in July 2009. This cold anomaly weakens as latitude increases and diminishes in high latitudes. In contrast to 2009, it is also worth noting that 2002 is an anomalously warm year, with a positive anomaly throughout the season. The histograms in Figure 9 indicate that the 0-D cloud number

anomaly and temperature anomaly are strongly anti-correlated throughout the season, which further supports a temperature control of cloud number variation. However, we note that at certain times around the start and end of the summer although the temperature anomaly is negative there are no clouds. This is simply because these cold anomalies occurred before the cloud season started or after it ended. At last, the strong agreement between the SABER and MLS anomalies during their overlapping period enhances the credibility of these variabilities, although in a later discussion we will find that the actual temperature values of SABER and MLS are biased from each other.

It requires further investigation to understand why the cold temperature in the core of the season is more stable. One hypothesis is that the existence of a large number of ice particles may stabilize the temperature. For example, Hervig et al. [2010] proposed ice temperature to describe the thermal state of the mesosphere when PMCs are present [also see Petelina et al., 2009]. Ice temperature is about 20-30K lower than the air temperature, and remains nearly constant during the time when ice is present.

6. Cloud lower boundary

Along with the finding that the lower latitude cloud number is increasing, we also wonder whether the mesospheric cloud low-latitude boundary is shifting southward systematically. The latter would suggest more extensive climate change in the mesosphere. Figure 9left and right show the latitude vs. time maps of the saturation vapor pressure, i.e., P_{SAT} , on 1-day vs. 5°-latitude grids. For each given day and each latitude bin the lowest P_{SAT} value is chosen. The white dots represent the first cloud run into when moving from 40°N toward higher latitude, marking the low-latitude boundary of the mesospheric clouds throughout the season. We note that P_{SAT} has shown a very sharp decrease across the cloud boundary, suggesting that temperature

controls the cloud boundary variation. Both SABER and MLS results support this argument. However, we find that prior to 20 DFS the boundaries indicated in the SABER and MLS analyses basically agree, with SABER boundary showing slightly more variability. While after DFS 20 toward the end of the season SABER shows far more southward boundary than MLS, pointing to colder SABER temperature on these latitudes. Remember that we just showed that temperature anomalies in these latitudes and time periods agree well between the two datasets. There is a possibility that SABER just captures more wave activities that have extended the seasonal length on these latitudes. Neilsen et al. [2010] used NOGAPS-ALPHA temperature and CIPS/AIM PMC data to verify that 5-day planetary waves have extended the PMC season in high polar latitude regions. Whether such a theory also applies to the mid-latitude region requires further investigation.

Yearly anomalies of the low-latitude boundary for running 8-day running windows are shown in Figure 10 left and middle panels, for SABER and MLS analyses, respectively. First of all we note a striking resemblance between the variations in the colored map and the previously shown temperature anomalies (Figure 9), which further supports the argument that the low-latitude cloud boundary is controlled by temperature. A similar trend analysis is performed for the cloud boundary anomaly and is shown in Figure 11 right panel. It indicates an apparent downward trend and the same inter-annual variability as in the temperature anomalies. However, the downward trend is extremely weak, reaching only $0.1^{\circ}/\text{yr}$, with a poor confidence level. Figure 11 overall indicates that low-latitude boundary shows qualitatively consistent results with the cloud numbers but its decadal trend is not statistically significant.

7. Role of H₂O in the cloud number variations

The role of H₂O in controlling the cloud number or frequency variations is considered minor, but this situation will change when only the bright clouds are counted. Figure 12 shows the yearly time series of 0-D cloud number for threshold 60ng/m³ in latitude bands 70°-75°N, 75°-80°N, and 80°-85°N. The lower latitudes are not shown because the clouds brighter than 60ng/m³ only exist for higher latitudes. Unlike what is shown in Figure 5, results in Figure 12 clearly indicate that SABER and MLS analyses show qualitatively different variabilities; SABER cloud number still shows basically the same trend as shown in Figure 5 because the H₂O condition used in SABER analysis remained unchanged over the years, while the upward trend shown in the MLS analysis is apparently caused by the H₂O variability. Remember that the upward H₂O trend shown in Figure 4 lower panels has a poor confidence level, but at this point the number of the 0-D modeled bright clouds shows a significant upward trend with a confidence level of 80-90%. This is because the number of bright clouds does not respond linearly to the mean H₂O level change. What is shown in Figure 12 reminds us to use caution when concluding whether H₂O takes a key role in the cloud number or frequency variation since the threshold for cloud detection might be critical. Note that such a threshold is not determined in actual PMC measurements, while 60ng/m³ is just a 0-D threshold that probably far exceeds the realistic magnitude. We have known from the previous studies that 0-D model over-estimates the ice mass but the extent of overestimation has not yet been evaluated.

8. Conclusions and discussions

Over the last decade the number of mesospheric cloud sightings in the mid-latitude region is increased. The most southward sightings have reached 37.2°N. The 10-year SABER/TIMED temperature and 7-year MLS/Aura temperature and H₂O are used to simulate

the mesospheric clouds and to interpret the increase of the cloud number. The model results indicate that on the yearly basis the number of the 0-D modeled clouds shows an upward trend with a high confidence level (~80-95%) in latitude range 40° - 55° N, although there is no systematic southward shifting of the low-latitude cloud boundary. It was also found that a significant decadal cooling trend exists in SABER temperature in the same latitude range, which is considered the primary driver to the cloud number increase. Inter-annually, SABER and MLS analyses show strong agreement throughout 2005-2011, lending support to the reliability of SABER temperature trend.

A 0-D thermal equilibrium mesospheric cloud model [Hervig et al., 2009] is used to perform the simulations. 0-D model proved highly effective in reproducing the intra-seasonal variations of cloud frequency and ice mass density [Rong et al., 2012]. In this paper we further verified that the local time dependence shown in the SHIMMER/STPSat-1 PMC dataset can also be well reproduced although the magnitudes of the cloud number differ. In this experiment temperature and H₂O data were taken from an assimilated dataset NOGAPS-ALPHA that used both SABER and MLS temperature to generate the 3D fields on four UT times. For different ice mass density thresholds, the overall modeled cloud numbers differ, but the local time dependence is robust and consistent for all the thresholds used. The 0-D model can faithfully reproduce the cloud variation on many different time scales because the responding time of the clouds to temperature and H₂O is as short as a few hours. Aside from validating the 0-D model, the excellent agreement between model results and observations also indicates that the diurnal variation of the SHIMMER PMCs reflects the local time dependence of temperature.

The mid-latitude cloud number increase over the last decade is driven by temperature rather than H₂O because the cloud frequency variation is primarily driven by temperature. For

example, the upward trend of the MLS H₂O in the high polar latitudes (Figure 4 lower panels) plays no role in the cloud number variations, i.e., both MLS and SABER results show a zero trend in these latitudes. Remember that the two sets of simulations used different H₂O conditions.

As latitude increases, the decadal trend of cloud number weakens significantly. Especially, in high polar latitudes the cloud number remains roughly constant. This is expected because under highly saturated condition, i.e., temperature is far below the frost point, the cloud frequency is close to 100% and there is no room for further increase, and the temperature control of cloud frequency no longer holds. Yet temperature in the polar latitudes also show significantly weakened trend. While solar cycle could have been a main driver of the intra-decadal variation in temperature, which appears to be the case for latitude range 40°-55°N, on polar latitudes there is no solar cycle signal shown in the temperature variation, the cause of which requires further investigation.

Yearly anomalies of cloud number and temperature are strongly anti-correlated throughout the cloud season, which further supported the temperature control of the cloud number variation. The anomalies of both cloud number and temperature are distinctly large on lower latitudes, but they are gradually diminished in polar latitudes, especially in the core of the season. This is consistent with the above finding that on the polar latitudes the temperature trend is extremely weak. The reduced anomaly and decadal trend in the high polar latitudes and in the core of the season may suggest that a large number of ice cloud particles have somewhat stabilizing effect on the air temperature.

This study can be further improved through obtaining longer records of PMCs, temperature, and H₂O, and properly interpreting the possible solar cycle dependence on the

latitude. While being able to use multiple datasets with longer records is the key point of achieving all these goals, it is known to be an extremely challenging task. Currently only a few satellite instruments take measurements in the mesosphere, and neither of them has been operating far beyond a decade. Efforts will be made to assimilate the different datasets to generate longer time series. Other options may include carrying out the current satellite missions into a longer future.

Acknowledgements:

We thank SABER team in GATS, Newport News, Virginia, and MLS team in JPL in Pasadena, California, respectively, for providing their data products through online resources. We also thank many OSIRIS/Odin team members who have retrieved different versions of OSIRIS PMCs over the years. We especially thank Mike Stevens and David Siskind for providing NOGAPS-ALPHA and SHIMMER datasets in a timely manner; furthermore, their invaluable advice on the data usage is critical to the accomplishment of this work. The appreciation is extended to many individuals that developed NOGAPS dataset over the years. This project is supported by SABER/TIMED mission and AIM mission funded by NASA.

References:

Baumgarten, G., A. Chandran, J. Fiedler, P. Hoffmann, N. Kaifler, J. Lumpe, A. Merkel, C. E. Randall, D. Rusch, and G. Thomas (2012), On the horizontal and temporal structure of noctilucent clouds as observed by satellite and lidar at ALOMAR (69N), *Geophys. Res. Lett.*, 39, L01803, doi:10.1029/2011GL049935.

Beig, G., et al. (2003), Review of mesospheric temperature trends, *Reviews of Geophysics*, 41, 4 / 1015 2003, doi:10.1029/2002RG000121.

Benze, S., C. E. Randall, M. T. DeLand, G. E. Thomas, D. W. Rusch, S. M. Bailey, J. M. Russell III, W. McClintock, A.W. Merkel, C.Jeppesen (2009), Comparison of polar mesospheric cloud measurements from the Cloud Imaging and Particle Size experiment and the solar backscatter ultraviolet instrument in 2007, *J. Atmos. Solar-Terr. Phys.*, vol. 71-3, 365-372, doi: [10.1016/j.jastp.2008.07.014](https://doi.org/10.1016/j.jastp.2008.07.014)

Berger, U., and F.-J. Lübken (2011), Mesospheric temperature trends at mid-latitudes in summer, *Geophys. Res. Lett.*, 38, L22804, doi: [10.1029/2011GL049528](https://doi.org/10.1029/2011GL049528).

Eckermann, S.D., K.W. Hoppel,, L., Coy, J.P. McCormack, D.E. Siskind, K. Nielsen, A. Kochenash, M. H. Stevens, C. R. Englert (2009), High-altitude data assimilation system experiments for the Northern Hemisphere summer mesosphere season of 2007. *J. Atmos. Solar-Terr.* 71, 531–551, doi: [10.1016/j.jastp.2008.09.036](https://doi.org/10.1016/j.jastp.2008.09.036).

Fiedler, J., Baumgarten, G., Berger, U., Hoffmann, P., Kaifler, N., and Lübken, F.-J.(2011), NLC and the background atmosphere above ALOMAR, *Atmos. Chem. Phys.*, 11, 5701-5717, doi:10.5194/acp-11-5701-2011.

Gadsden, M. (1998), The North-West Europe data on noctilucent clouds: a survey, *J. Atmos. Solar-Terr. Phys.*, 60-12, 1163-1174.

Garcia, R. R., D. R. Marsh, D. E. Kinnison, B. A. Boville, and F. Sassi (2007), Simulation of secular trends in the middle atmosphere, 1950–2003, *J. Geophys. Res.*, 112, D09301, doi: [10.1029/2006JD007485](https://doi.org/10.1029/2006JD007485).

Hervig, M., and D. Siskind (2006), Decadal and inter-hemispheric variability in polar mesospheric clouds, water vapor, and temperature, *J. Atmos. Solar-Terr. Phys.*, doi:10.1016/j.jastp.2005.08.010.

Hervig, M. E., M. H. Stevens, L. L. Gordley, L. E. Deaver, J. M. Russell, and S. Bailey, Relationships between PMCs, temperature and water vapor from SOFIE observations (2009), *J. Geophys. Res.*, 114, D20203, doi:10.1029/2009JD012302.

Hervig, M. E., and L. L. Gordley (2010), Temperature, shape, and phase of mesospheric ice from Solar Occultation for Ice Experiment observations, *J. Geophys. Res.*, 115, D15208, doi:10.1029/2010JD013918.

Kirkwood, S., P. Dalin, and A. Rěchou (2008), Noctilucent clouds observed from the UK and Denmark – trends and variations over 43 years, *Ann. Geophys.*, 26, 1243-1254.

Lambert, A., et al. (2007), Validation of the Aura Microwave Limb Sounder middle atmosphere water vapor and nitrous oxide measurements, *J. Geophys. Res.*, 112, D24S36, doi:10.1029/2007JD008724.

Llewellyn, E.J., et al. (2004), The OSIRIS instrument on the Odin spacecraft, *Canadian Journal of Physics* 82, 411–422.

Lübken, F.-J. (2000), Nearly zero temperature trend in the polar summer mesosphere, *Geophys. Res. Lett.*, 27, 3603–3606.

Meinel A. B., B. Middlehurst, E. Whitaker (1963), Low-Latitude Noctilucent Cloud of 15 June 1963, *Science*, 1963 Sep 20;141(3586):1176-8.

Nielsen, K., D.E. Siskind, S.D. Eckermann, K.W. Hoppel, L. Coy, J.P. McCormack, S. Benze, C.E. Randall, and M.E. Hervig, Seasonal variation of the quasi 5-day planetary wave: Causes and consequences for polar mesospheric cloud variability in 2007 (2010), *J. Geophys. Res.* 115, D18111, doi:10.1029/2009JD012676.

Nielsen, K., Nedoluha, G. E., Chandran, A., Chang, L. C., Barker-Tvedtnes, J., Taylor, M. J., Mitchell, N. J., Lambert, A., Schwartz, M. J. and Russell, J. M. (2011), On the origin of mid-latitude mesospheric clouds: The July 2009 cloud outbreak. *Journal of Atmospheric and Solar-Terrestrial Physics*, 73 (14-15), pp. 2118-2124.

Petelina, S., E. J. Llewellyn, D. A. Degenstein, N. D. Lloyd (2006), Odin/OSIRIS limb observations of polar mesospheric clouds in 2001-2003, *J. Atmos. Solar Terr. Phys.*, 68, doi:10.1016/j.jastp.2005.08.004.

Petelina, S., E. J. Llewellyn, and D. A. Degenstein (2007), Properties of polar mesospheric clouds measured by ODIN/OSIRIS in the northern hemisphere in 2002-2005, *Can. J. Phys.*, 85, 1143–1158, doi:10.1139/P07-092.

Petelina, S. V., and A. Y. Zasetsky (2009), Temperature of mesospheric ice retrieved from the O-H stretch band, *Geophys. Res. Lett.*, 36, L15804, doi:10.1029/2009GL038488.

Remsberg, E. E., *et al.* (2008), Assessment of the quality of the Version 1.07 temperature-versus-pressure profiles of the middle atmosphere from TIMED/SABER, *J. Geophys. Res.*, 113, *D17101*, doi:[10.1029/2008JD010013](https://doi.org/10.1029/2008JD010013).

Remsberg, E. E. (2009), Trends and solar cycle effects in temperature versus altitude from the Halogen Occultation Experiment for the mesosphere and upper stratosphere, *J. Geophys. Res.*, 114, *D12303*, doi:[10.1029/2009JD011897](https://doi.org/10.1029/2009JD011897).

Remsberg, E. (2010), Observed seasonal to decadal scale responses in mesospheric water vapor, *J. Geophys. Res.*, 115, *D06306*, doi:[10.1029/2009JD012904](https://doi.org/10.1029/2009JD012904).

Rong, P., J. M. Russell III, S. M. Bailey, and M. E. Hervig, The roles of temperature and water vapor at different stages of the PMC season, *J. Geophys. Res.* 117, *D4*, doi:10.1029/2011JD016464, 2012.

Russell, J. M., III, L. L. Gordley, J. H. Park, S. R. Drayson, D. H. Hesketh, R. J. Cicerone, A. F. Tuck, J. E. Frederick, J. E. Harries, and P. Crutzen (1993), The halogen occultation experiment, *J. Geophys. Res.*, 98(D6), 10,777–10,797, doi:10.1029/93JD00799.

Russell, J. M. III, P. Rong, S. M. Bailey, M. E. Hervig, and S. V. Petalina, Relationship between the Summer Mesopause and Polar Mesospheric Cloud Heights (2010), *J. Geophys. Res.*, 115, D16209, doi:10.1029/2010JD013852.

Schwartz, M. J., et al. (2008), Validation of the Aura Microwave Limb Sounder temperature and geopotential height measurements, *J. Geophys. Res.*, 113, D15S11, doi:10.1029/2007JD008783.

Siskind, D. E., M. H. Stevens, M. Hervig, F. Sassi, K. Hoppel, C. R. Englert, A. J. Kochenash (2011), Consequences of recent Southern Hemisphere winter variability on polar mesospheric clouds, *J. Atmos. Solar Terr. Phys.*, 73, 2013–2021, doi:10.1016/j.jastp.2011.06.014

Stevens, M.H., C. R. Englert, M. Hervig, S. V. Petalina, W. Singer, K. Nielsen (2009), The diurnal variation of polar mesospheric cloud frequency near 55°N observed by SHIMMER, *J. Atmos. Solar Terr. Phys.*, 71, 401–407, doi:10.1016/j.jastp.2008.10.009

Waters, J. W., et al. (2006), The Earth Observing System Microwave Limb Sounder (EOS MLS) on the Aura satellite, *IEEE Trans. Geosci. Remote Sensing* 44, no. 5.

Wickwar, V. B., M. J. Taylor, J. P. Herron, and B. A. Martineau (2002), Visual and lidar observations of noctilucent clouds above Logan, Utah, at 41.7°N, *J. Geophys. Res.*, 107(D7), 4054, doi:10.1029/2001JD001180.

Figure Captions:

Figure 1: The NLC sightings in the United States during northern summers of 2003, 2007, 2008, and 2009 recorded by space-weather archived NLC gallery. The 33 sightings, which mainly

occurred in July in about 8 states and 26 cities, are shown. Some of the earlier sightings, such as those observed in Utah in 1999, are not included. The black dots are for years other than 2009, and large circles are for 2009 only, and the latitudinal circles (dotted) are 50°N, 60°N, 70°N, and 80°N.

Figure 2: (Upper) OSIRIS PMC daily appearance frequency in latitude range 40°-85°N. (Lower) 0-D modeled PMC daily frequency in the same latitude range. MLS temperature and H₂O profiles are used in the 0-D simulation. Note that all 0-D model simulations in this paper are performed on the pressure level 0.00464 hPa.

Figure 3: Daily cloud number variations of 0-D model results and SHIMMER PMCs. The 0-D clouds are simulated on the SHIMMER orbital tracks using NOGAPS-ALPHA assimilated temperature and H₂O, and the latitude range is confined to 50°-58°N. The 0-D results are shown for different ice mass density thresholds, i.e., 0, 25, and 40 ng/m³.

Figure 4: (Upper-left) MLS H₂O 7-year climatology based on the daily zonal maximum values. (Upper-right) same as the left panel except for using the zonal mean rather than maximum. (Lower-left) Inter-annual variability and secular trend of H₂O on pressure level 0.00464 hPa. The yearly values are obtained through calculating the mean of all the data points in a given latitude band from 1 May to 31 August. (Lower-right) Same as the left panel except for using only the data points in the core of PMC season from the summer solstice to 25 days after the solstice (DFS).

Figure 5: Inter-annual variability and the secular trend of the 0-D simulated cloud numbers in different latitude bands, with a 5-degree increment. The cloud number is normalized by the corresponding multi-year averages, denoted by N_{norm} . Note that the SABER 0-D results are from

simulations using SABER temperature and the MLS H₂O climatology shown in the upper-left panel of Figure 4.

Figure 6: Same as Figure 5 except that an adjusting factor is included, based on the fact that the event number varies slightly with year. The factor is defined as the current year event number divided by its multi-year average. It is mostly close to 1.0 because for both SABER and MLS there is only a small fluctuation in their event numbers from year to year. The normalized and then adjusted cloud number is denoted by N_{norm_adj} .

Figure 7: (Upper) Comparisons of 0-D modeled and OSIRIS cloud numbers in lower latitude bands. Since the overall numbers between the two sets are drastically different, both variables are subtracted the corresponding mean and then are divided by their standard deviations. (Lower-left) N_{norm_adj} for 0-D MLS PMCs. (Lower-right) N_{norm_adj} for OSIRIS PMCs. Adjusting factor is particularly important for OSIRIS PMCs because the event number varies drastically from year to year, especially in 2005 and 2006 the event numbers are several times fewer than in the following years.

Figure 8: Inter-annual variability and the secular trend of SABER and MLS temperature. For each latitude band, the yearly value is obtained from calculating the average from 1st May to 31 August. The secular trend of MLS temperature is not indicated because the time series is quite a few years shorter than a decade and SABER temperature serves as a better guidance for an estimation of the decadal temperature trend.

Figure 9: Colored maps: intra-seasonal variations of the yearly temperature anomaly from the corresponding multi-year averages in different latitude bands and each 8-day running window. Histograms: temperature anomaly (pink) and cloud number (N_{norm}) anomaly (rainbow) are shown

together to indicate their apparent anti-correlations. The temperature anomaly range is set to -10K to 10 K, and the cloud number anomaly minimum and maximum are indicated inside each panel.

Figure 10: latitude vs. time maps of saturation vapor pressure (P_{SAT}). The white dots represent the low-latitude boundary of the 0-D PMCs. For a given day it is the latitude where the first cloud occurs north of 40°N. The low-latitude boundary coincides with the line across which there is a rapid decrease in P_{SAT} .

Figure 11: (Left and middle) same as Figure 10 except for the low-latitude boundary for PMCs. (Right) inter-annual variability and secular trend of the cloud boundary anomaly.

Figure 12: Same as Figure 5 except that only the brightest clouds ($>60\text{ng/m}^3$) are included. In this case SABER and MLS differ significantly because SABER used a constant H_2O climatology.

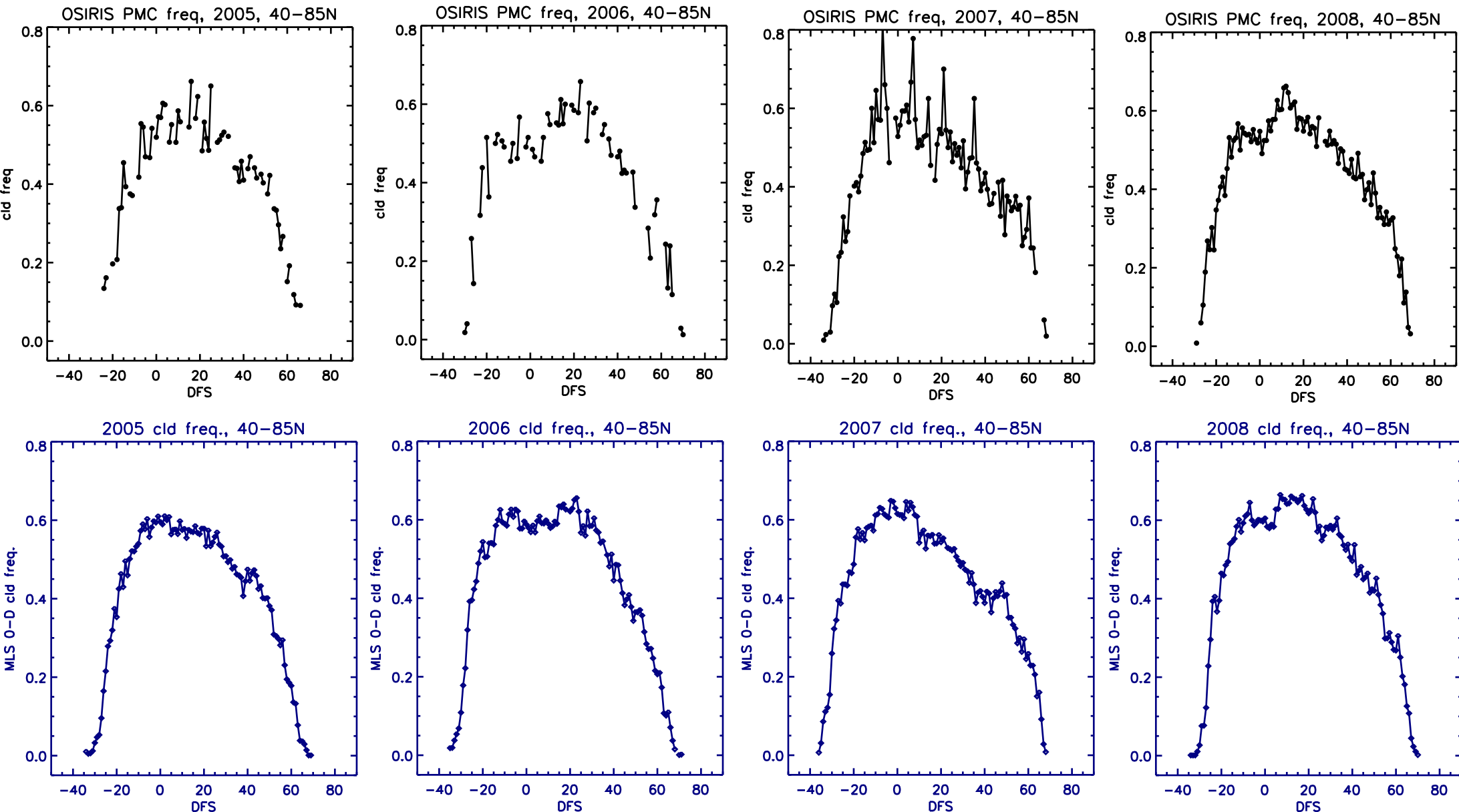
Fig. 2

Fig2-cont.

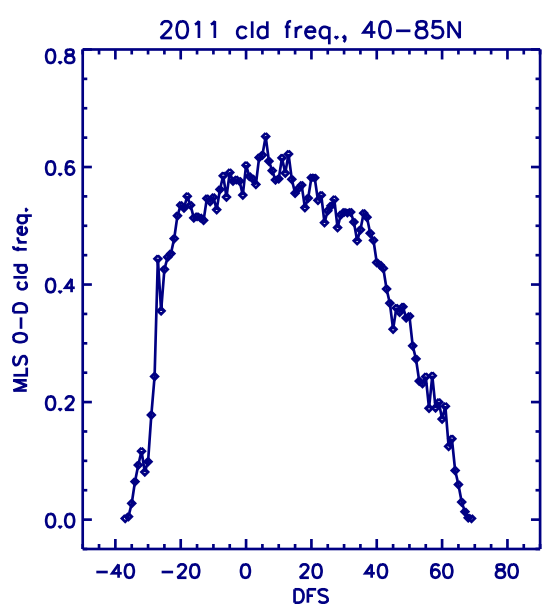
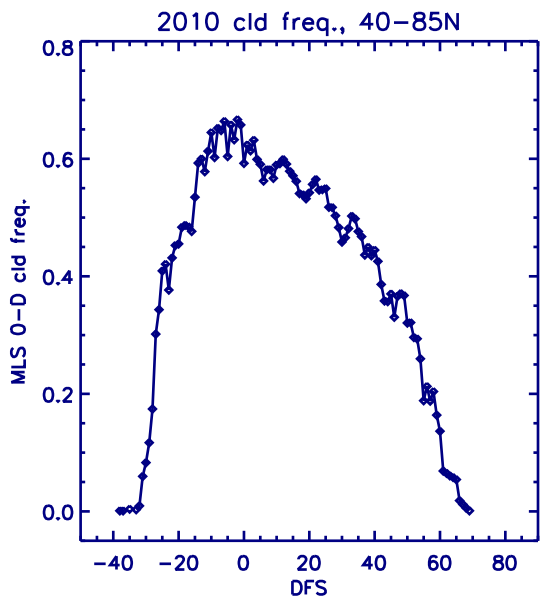
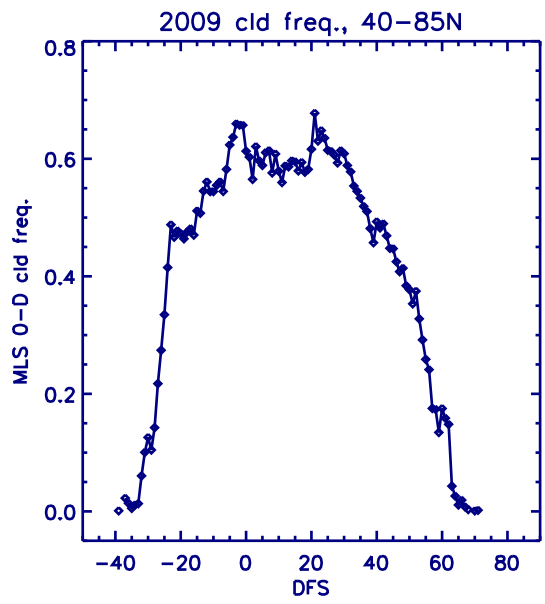
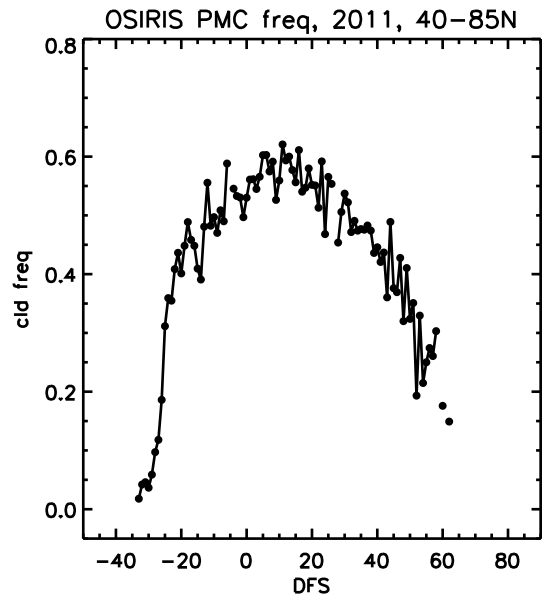
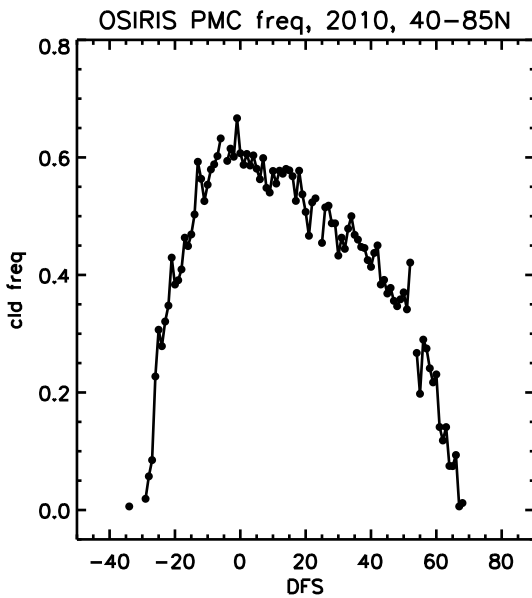
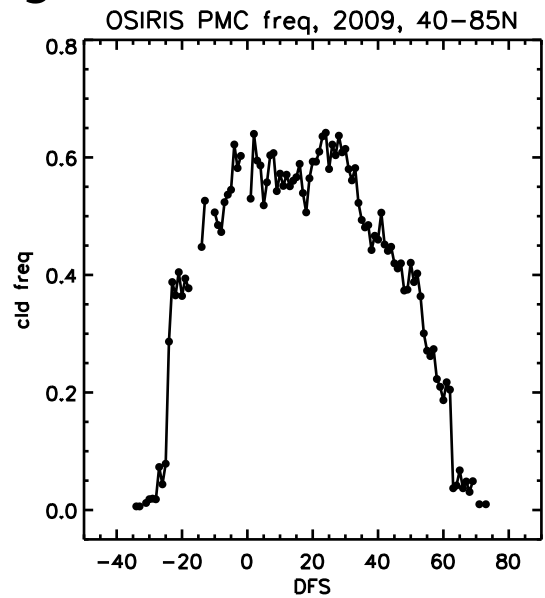


Fig.3

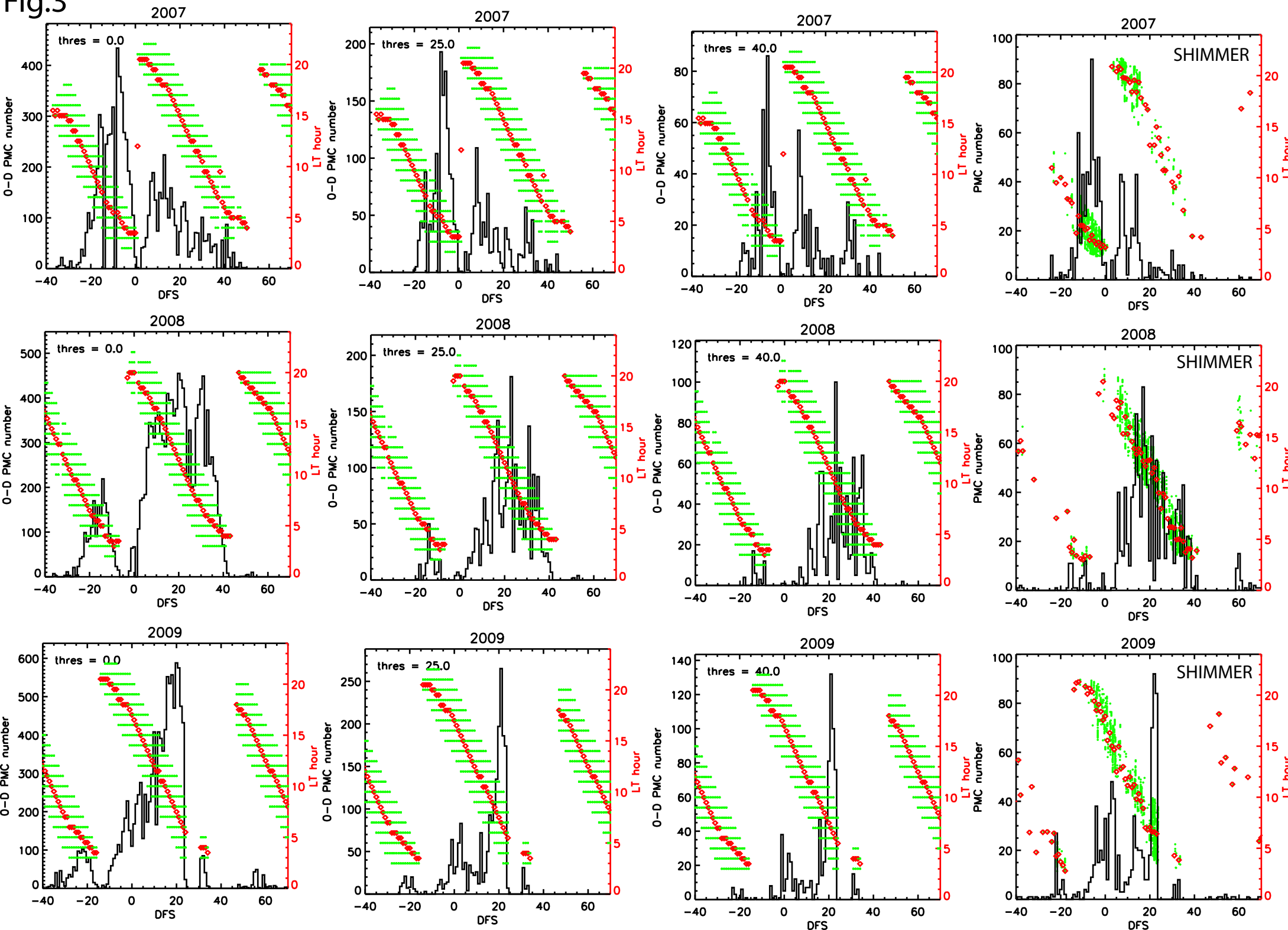
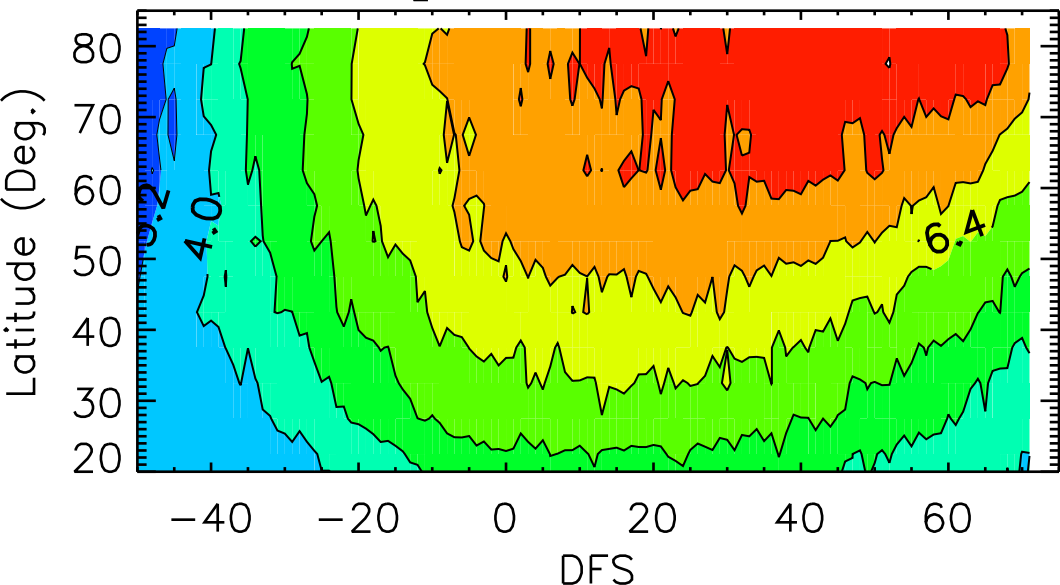
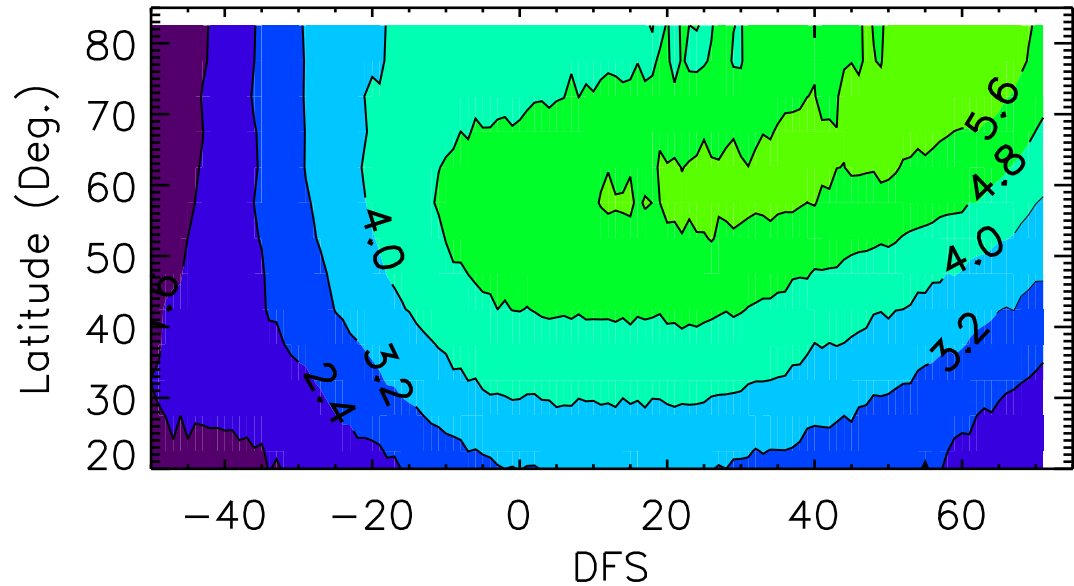


Fig. 4

H₂O_max climate



H₂O_m climate



DFS

DFS

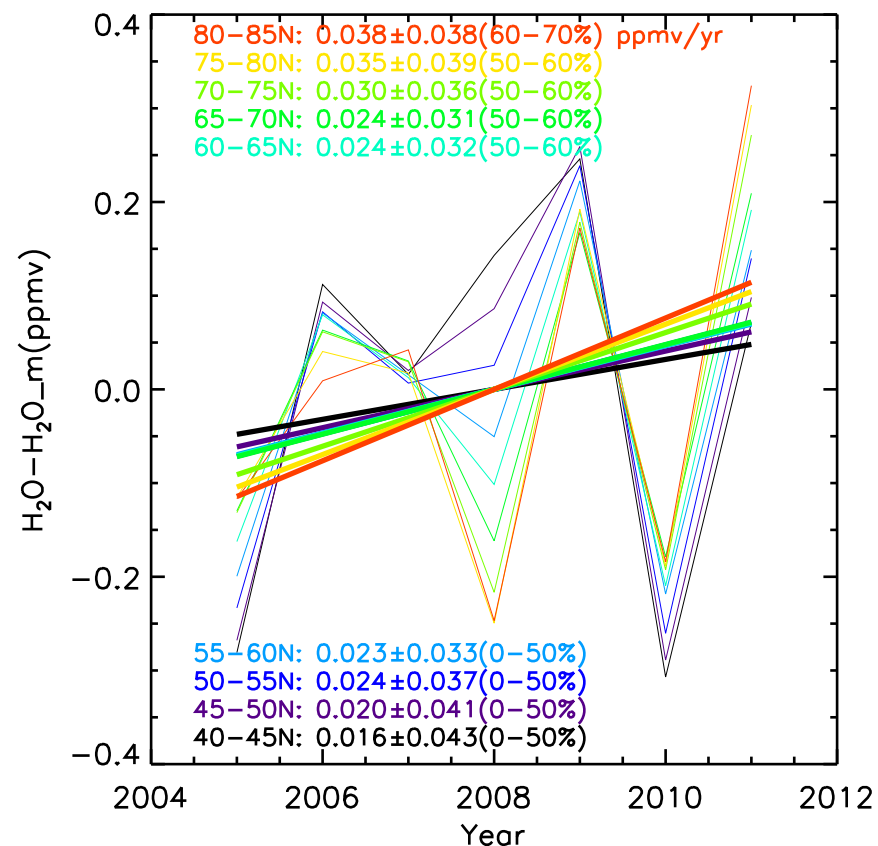
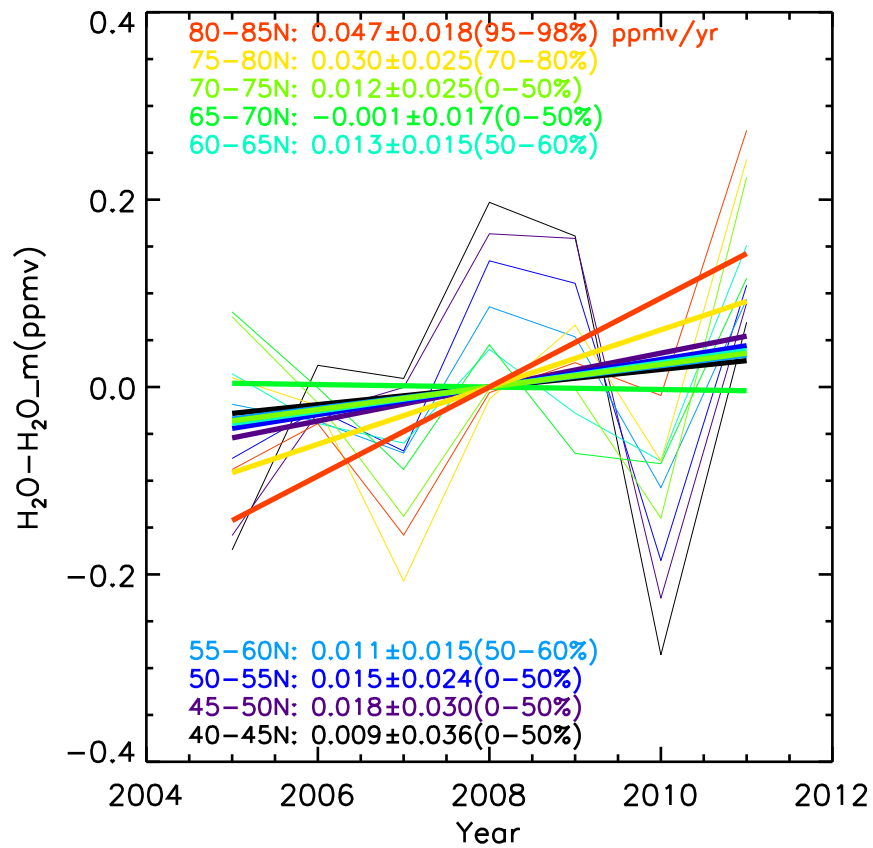


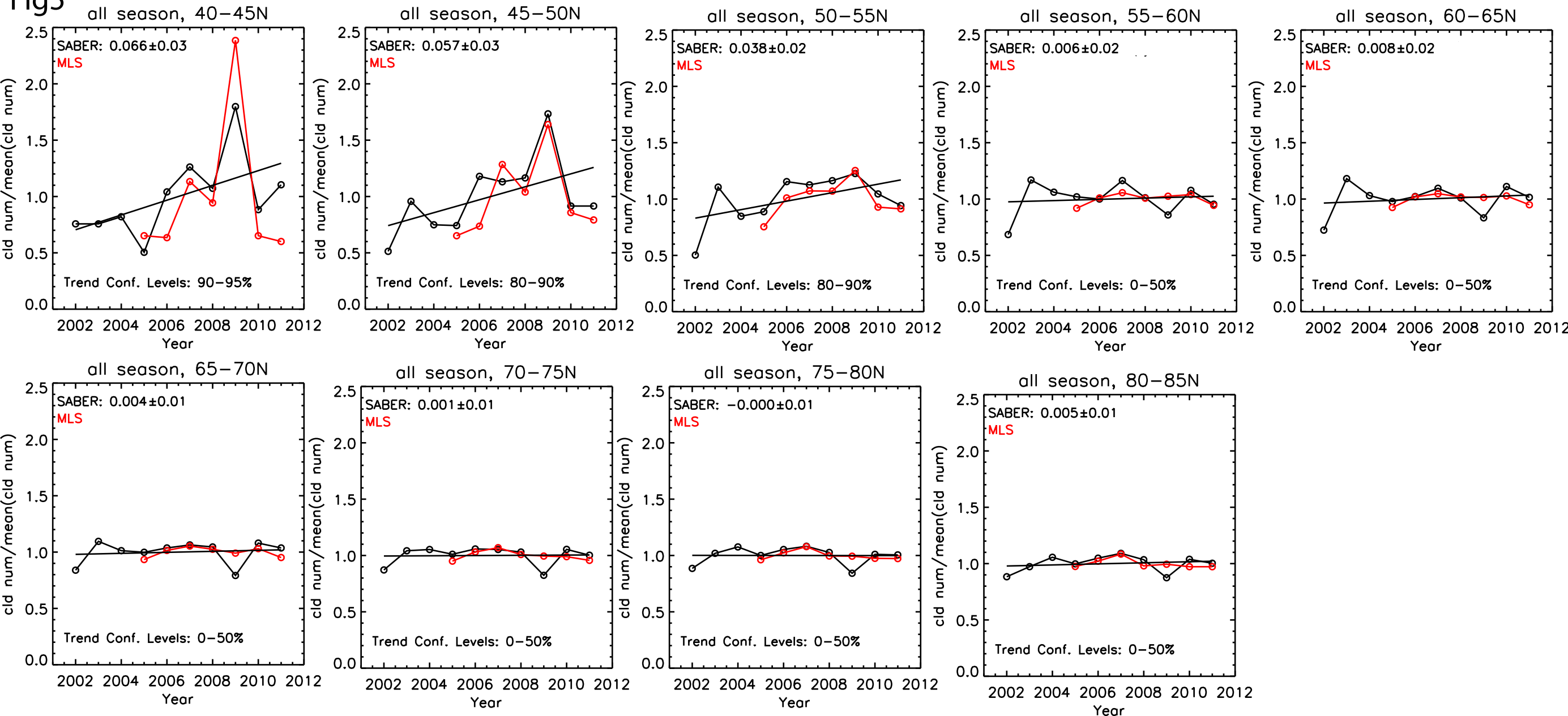
Fig5

Fig6

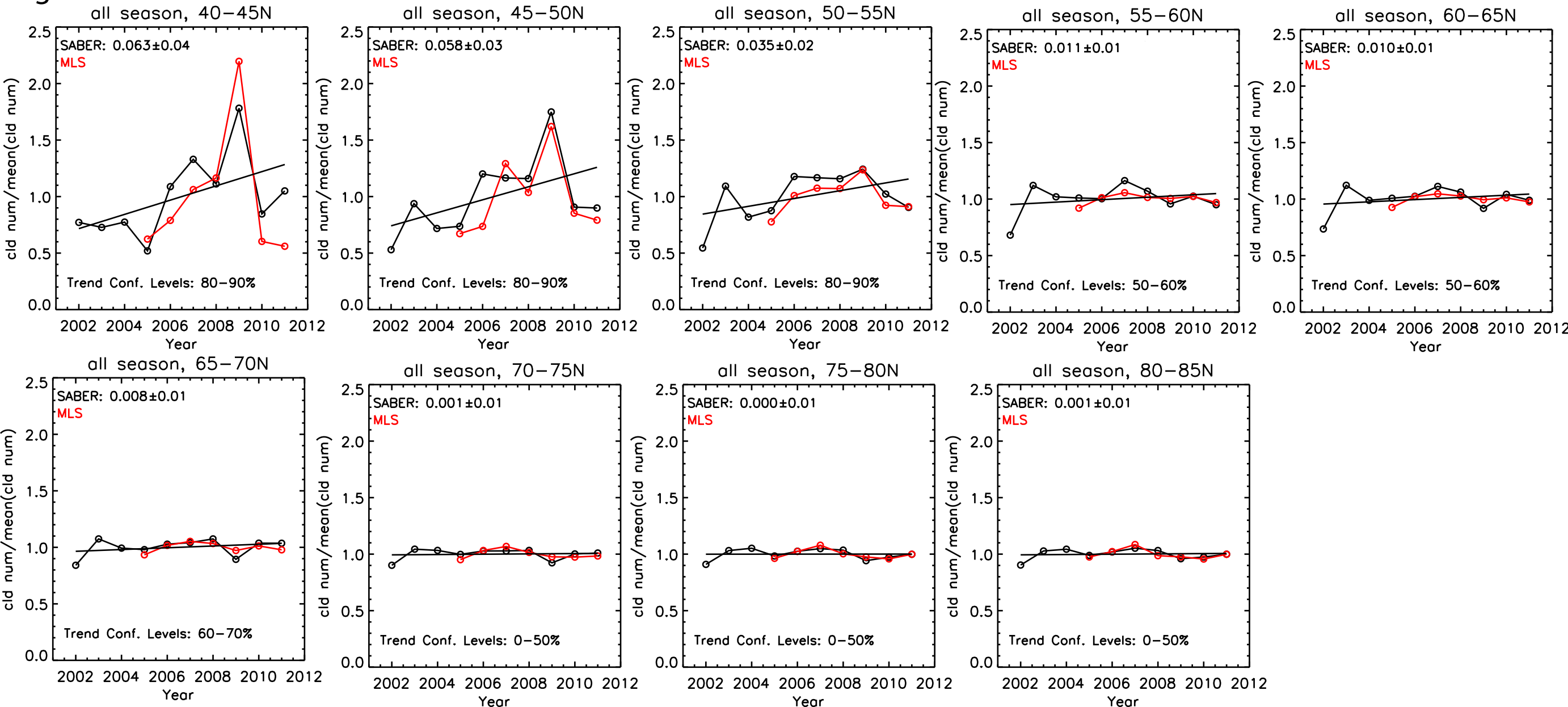
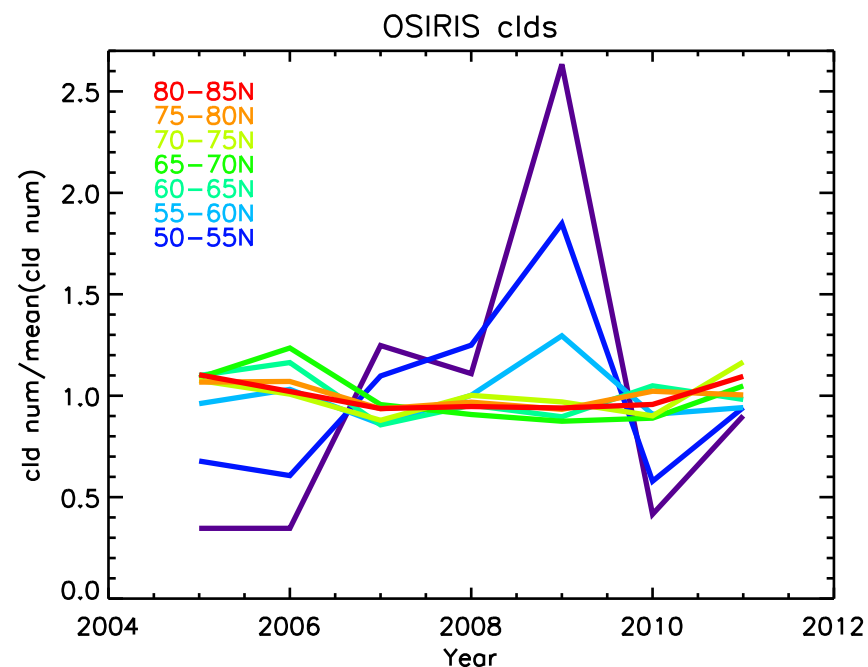
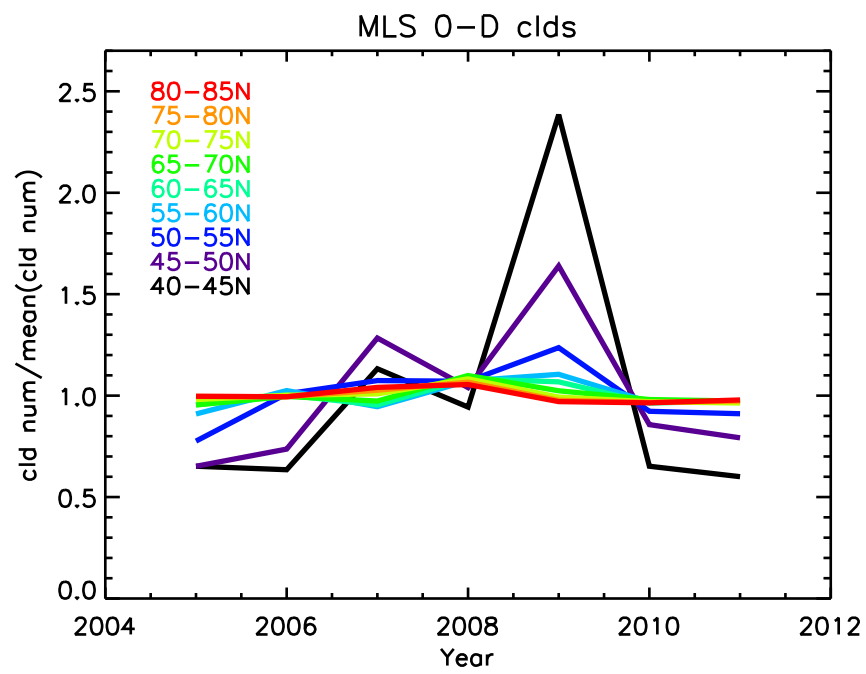
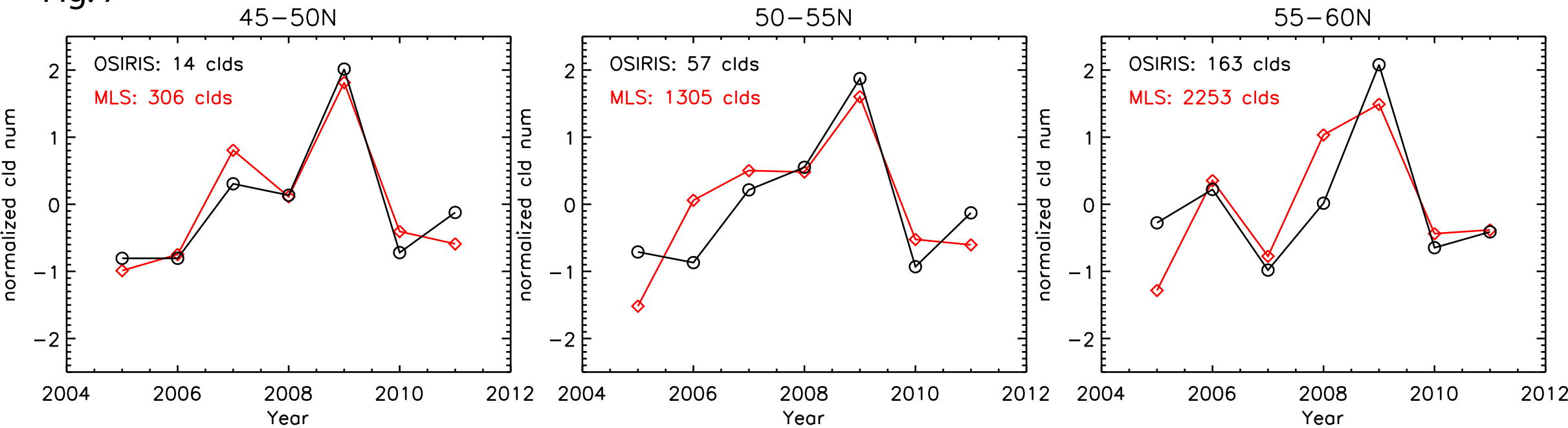


Fig. 7



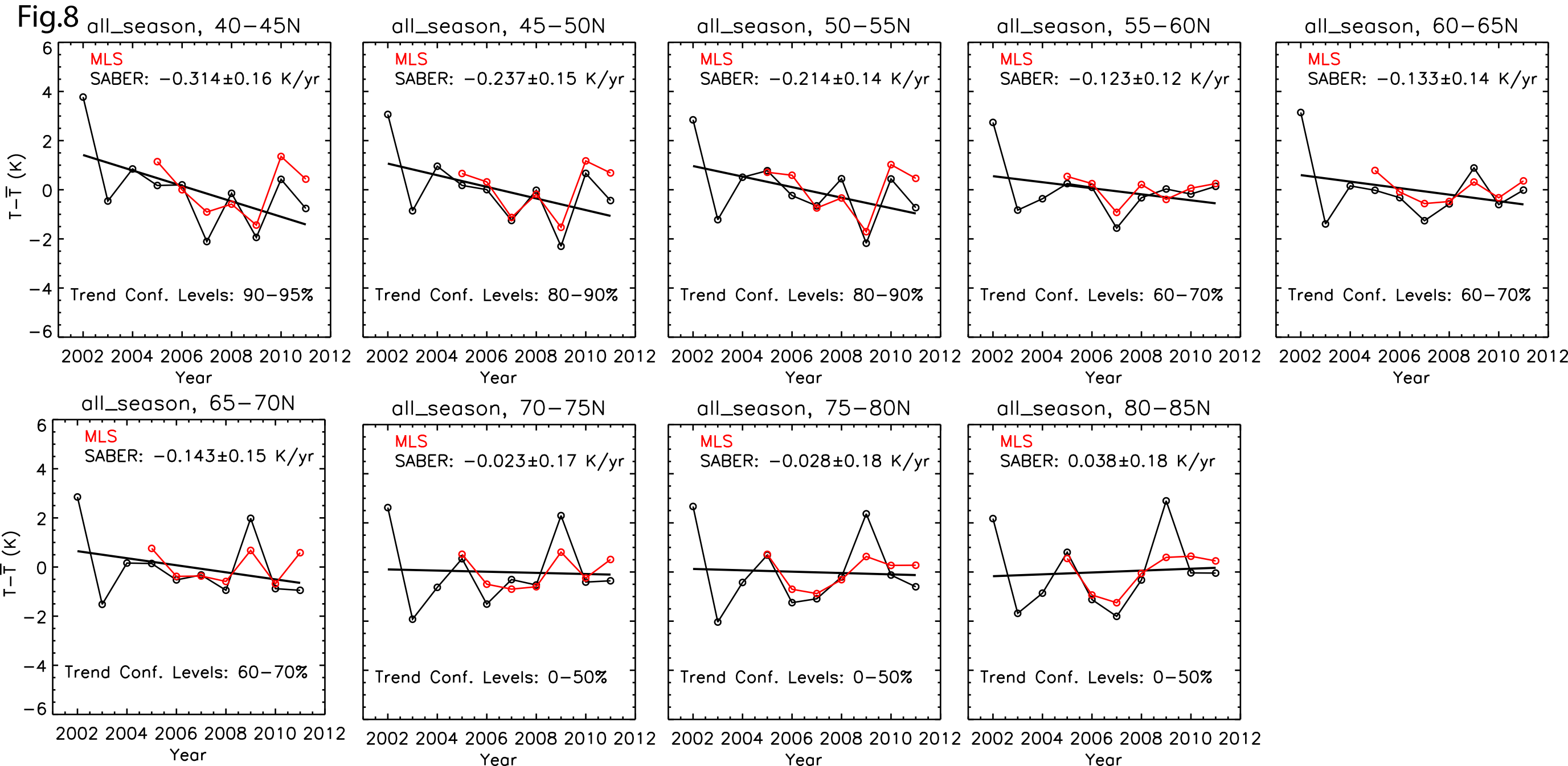


Fig. 9

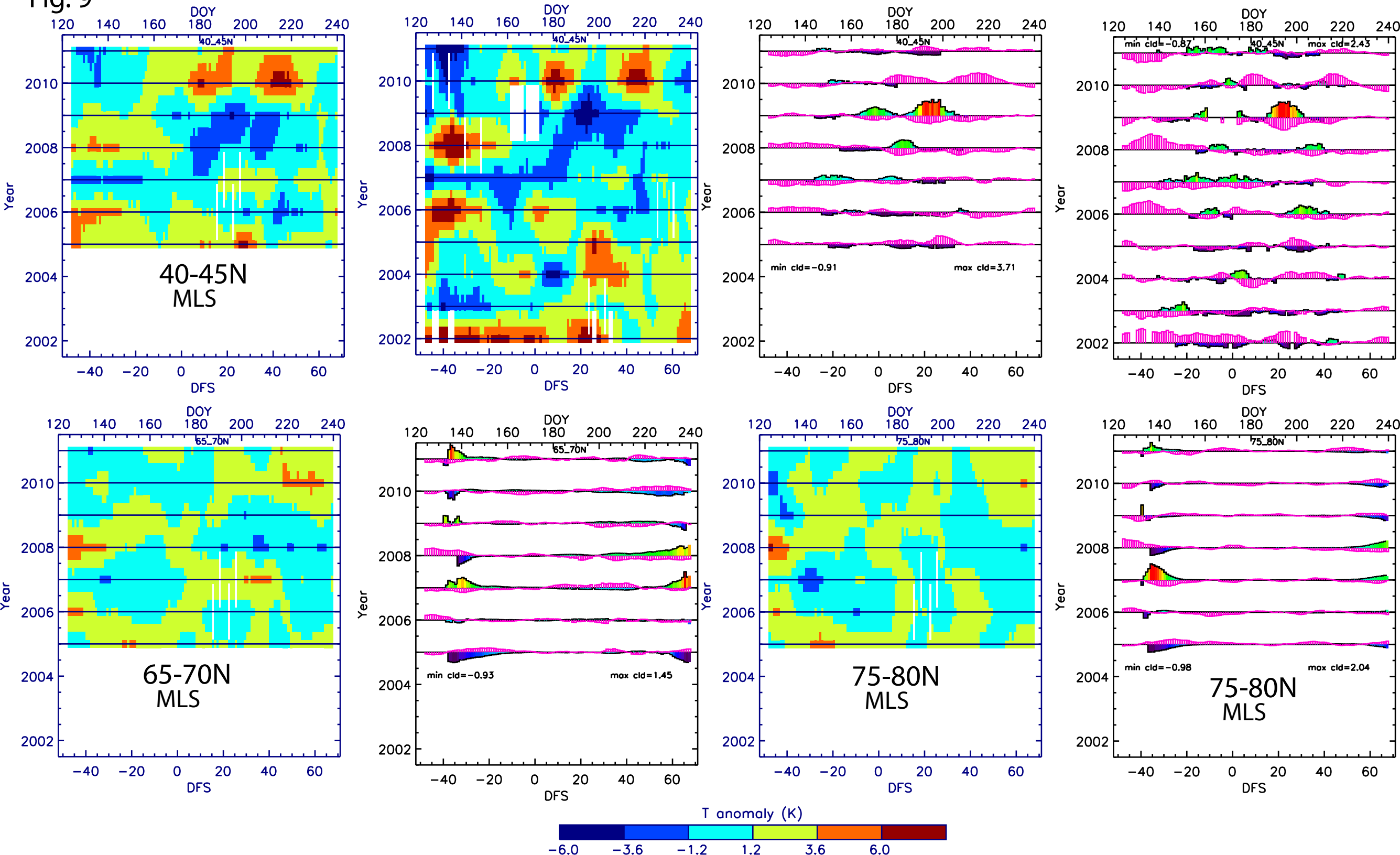


Fig. 10

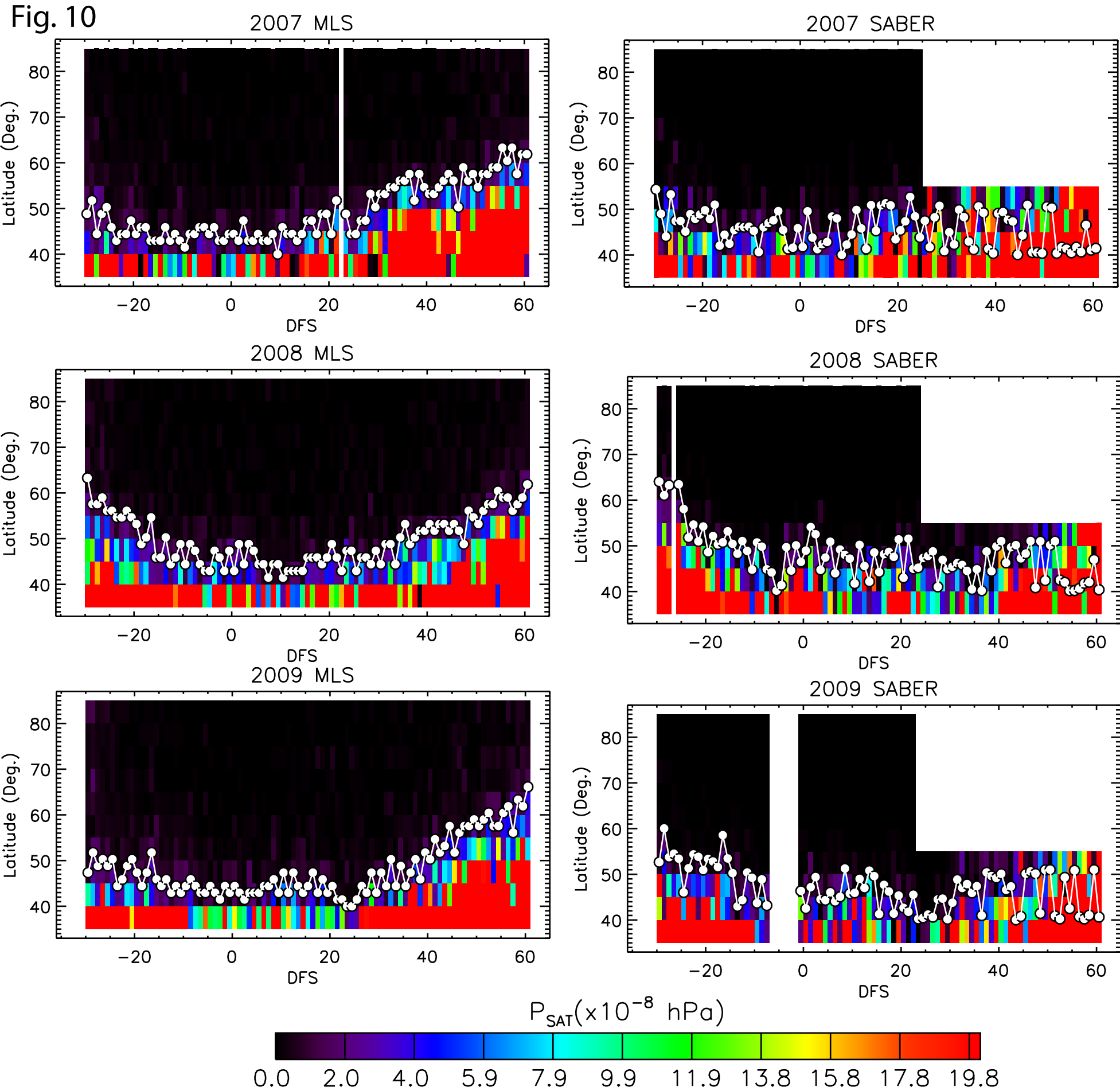
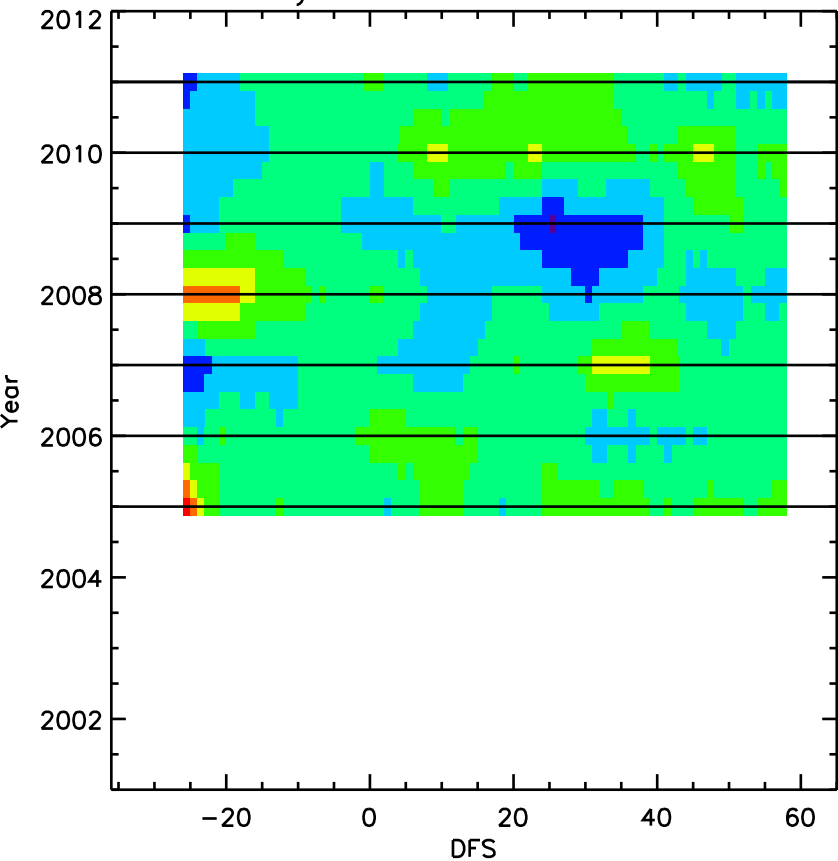
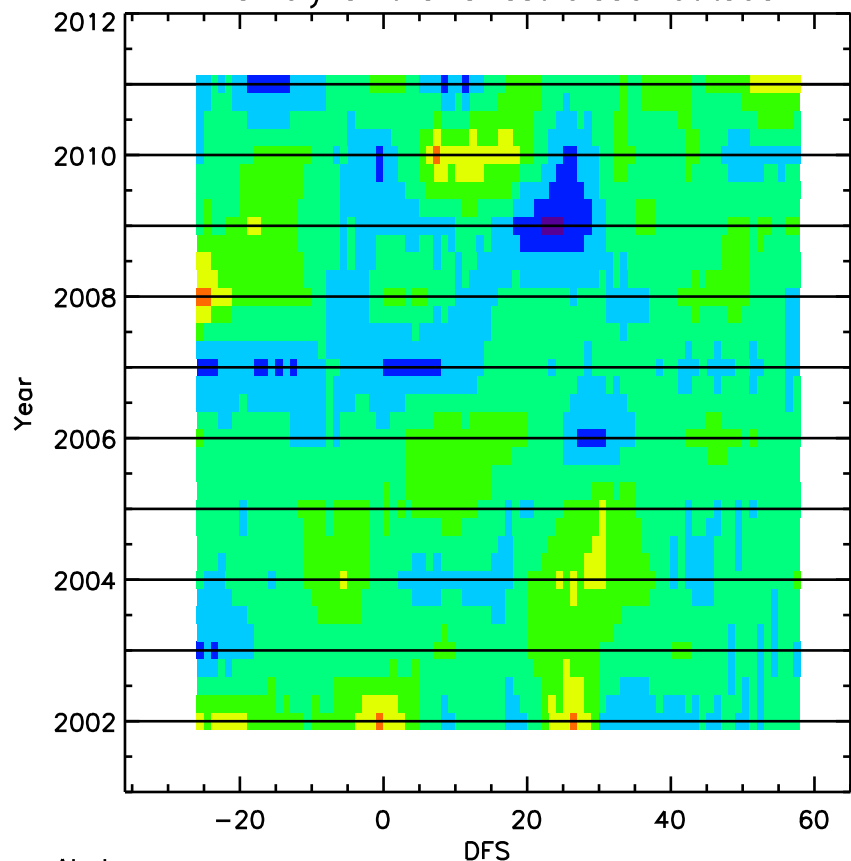


Fig. 11

Anomaly of the lowest cloud latitude



Anomaly of the lowest cloud latitude



seasonal mean of cld bndry anomaly (Deg.)

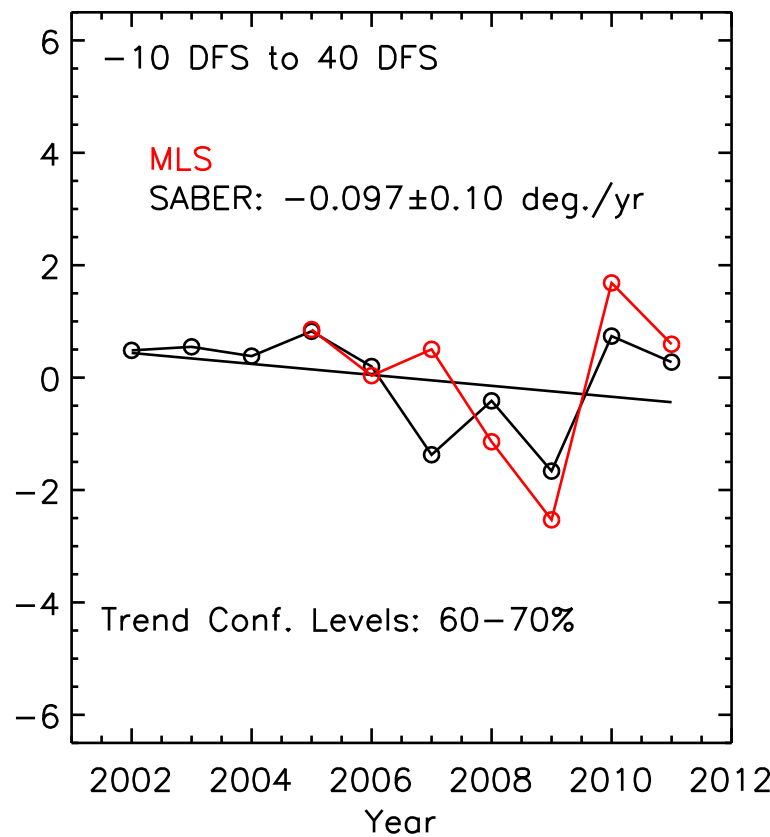


Fig. 12 cloud number trend for $m_{ice} > 60 \text{ ng/m}^3$

